THE EUROPEAN PHYSICAL JOURNAL PLUS

Thermoelectric, structural, electronic, magnetic, and thermodynamic properties of CaZn₂Ge₂ compound

Abdul Ahad Khan[1], Ali H. Reshak[2,3,a] , Zeshan Zada[4], Muhammad Saqib[5], Zeesham Abbas[6], Muhammad Ismail[6,7], Sabeen Zada[8], G. Murtaza[4,8], Shahid Ali[9], Amel Laref[10]

[1] Department of Physics, University of Peshawar, Peshawar 25120, Pakistan
[2] Physics Department, College of Science, University of Basrah, Basrah 61004, Iraq
[3] Center of Excellence Geopolymer and Green Technology (CEGeoGTech), University Malaysia Perlis, 01007 Kangar, Perlis, Malaysia
[4] Materials Modeling Lab, Department of Physics, Islamia College University, Peshawar 25120, Pakistan
[5] Department of Electrical and Computer Engineering, COMSATS University Islamabad, Abbottabad Campus, Abbottabad 22060, Pakistan
[6] Department of Nanotechnology and Advaced Materials Engineering, Sejong University, Seoul 05006, Republic of Korea
[7] Chemistry, Women Univeristy Swabi, Swabi, Khyber Pakhtunkhwa, Pakistan
[8] Department of Mathematics & Natural Sciences, Prince Mohammad Bin Fahd University, P. O. Box 1664, Alkhobar 31952, Kingdom of Saudi Arabia
[9] Institute of Materials, Shanghai University, Shanghai 200444, China
[10] Department of Physics and Astronomy, College of Science, King Saud University, Riyadh 11451, Kingdom of Saudi Arabia

Abstract The structural, electronic, magnetic, thermoelectric and thermodynamic properties of CaZn₂Ge₂ compound from zintl family was examined under the frame work of density functional theory (DFT). The optimization results indicated that the Ferromagnetic configuration is the stable one. From the band structure and electrical conductivity (σ/τ) calculations CaZn₂Ge₂ reveled metallic nature. The strong hybridization was observed between Ca-d and Ge-p states, whereas as a whole it showed mix ionic and covalent bonding nature. The reported low magnetic moments of the compound by and (GGA + U) approximations revealed weak ferromagnetism. Due to these unique properties, the material is promising for spintronics devices and magnetic applications. Furthermore for the calculation of thermoelctric properties the Boltztrap code was used in the temperature range from 0 to 1000 K. The maximum electrical conductivity (σ/τ) and negative seebeck coefficient (S) with the values $5.6 \times 10^{20} (\hat{\Omega}.m.s)^{-1}$ and -2.25×10^{-5} μV/K were reached below the room temerature while maximum ZT with a value 0.0171 and power factor were achieved at 1000 K. This finding increased the demand of use this material in waste heat management. Moreover, the thermodynamic properties for CaZn₂Ge₂ compound in the pressure range from 0 to 18GPa and temperature variation from 200 to 1400 K were discussed.

1 Introduction

Recently, the Zintl compounds have attracted incredible regard to explore their fascinating structural, electronic, elastic, optical, magnetic and thermoelectric properties [1–9]. Several compounds with general formula (AM₂X₂, A = rare-earth metals/alkaline-earth, M = mostly d-block transition metals; X = Group 13–16 elements) basically exist in two structural types, namely, ThCr₂Si₂ (I4/mmm) and CaAl₂Si₂ (P3̄m1) [10]. The well-known ThCr₂Si₂-type, first published in 1965 by Ban and Sikirica [11] is the crystal structure with many representatives. The main reasons for this are its possibility to adapt to strongly different atomic sizes as well as to a wide range of electron counts. Majority of ThCr₂Si₂-type compounds have attractive physical properties such as superconductivity [12], mixed valence [13], along with a wide range of magnetic effects [14–16].

Various zintl compounds have been extensively studied as intermetallics phase from the past few years [17–21], because of their scientific and technological outcome as "colossal" or "giant" magneto-resistive (CMR or GMR) materials in the broad range series of applications from computer read, shape memory alloys, dentistry and jewelry [22]. While magneto-resistance in metallic thin films is accomplished by changing the resistivity under the influence of an external magnetic field.

Nevertheless, about intermetallic phases there have been few reports that show both (G-M-R or C-M-R) at modest magnetic fields [23]. The GMR could be essentially utilized as spin filters, magnetic-field sensors and spin valves. While its other important usage in latest innovations apart from this could not be ignored, such as micro-electromechanical systems (MEMS), hard disk drives, magnetic and biosensors respectively [24, 25].

The structure of AM₂X₂ is developed by MX₄ tetrahedra (layers of negatively charged) and A (layers of positively charged), which are alternately stacked along [001]. The MX₄ layers have strong (M–X) covalent bonds along with weaker (M–M) interactions, whereas the bonding between A and the layers is ionic up to certain extent. Researchers on the other hand have reported [26] that

---

ᵃ e-mail: maalidph@yahoo.co.uk (corresponding author)

Springer

a single bonding scheme (covalent/metallic/ionic) cannot give a suitable complete explanation in ternary phosphides while using LMTO for band structure calculations. So mostly in these compounds all three kinds of bonding schemes are present. The accord between them can purpose instabilities which appear in (first/second-order) phase transitions induced by three different main factors such as pressure, temperature, and by substitution. The phase transitions are generally joined by strong changing in lattice parameters and especially of the (P–P) separation among the layers of MP_4 tetrahedra have been reported in various articles [27–32]

The synthesis and characterization of crystal structure of both new $CaZn_2Si_2$ and $EuZn_2Ge_2$ compounds along with the magnetic measurements and (Mossbauer spectroscopic) experiments of the europium based compound have been reported for the first time [1]. To comprehend the uncommon changes in the lattice parameters of CaM_2Ge_2 with M = Mn–Zn, an examination of chemical bonding dependent on LMTO band-structure computations have been presented in the same work. The transport properties of Zintl compounds have been reported by Jifeng and Singh [3]. Later on the electronic structure along with thermoelectric properties of associated compound were also investigated by both Franck et al.[4] and Eric et al. [6]. Furthermore forbidden gap of 0.33 eV was calculated for $CaZn_2Sb_2$ compound to have semiconducting nature in agreement with the measured energy gap of value (0.26 eV) [6]. When it comes to $CaZn_2Ge_2$ (space group *I4/mmm*) compound the tetrahedra ($ZnGe_4$) are almost undistorted. This is due to the closed Zn-3d shell connects virtually not with other connected orbitals. Thusly, no antibonding (Zn–Ge) states present close to the Fermi-level and a complete distortion of the tetrahedra (ZnGe4) would not make any increase in energy [1].

The experimental and theoretical approaches have been completed on the same family of different zintl compounds by many researchers to check their various physical properties, for the sack of their use in valuable applications and device fabrications [18–21, 33–35]. Among all these zintl compounds with important applications for device innovations zinc (Zn)-containing zintl compound $CaZn_2Ge_2$ is the most common and attarctive material and need further thorough investigation. Furthermore structure properties of the compound $CaZn_2Ge_2$ are only available, due to lack of the availability of the data about the rest of other physical properties need more attention for fruitful possible output. Reporting new materials and their examination for adjusting them is the most attractive area of research in present-days. There are no past combine data available on the remaining properties to the best of our knowledge, on First-principles calculations of structural, electronic, magnetic, thermoelectric and thermodynamic properties of $CaZn_2Ge_2$ compound.

2 Method of calculations

In this report, the computational data has been achieved for $CaZn_2Ge_2$ compound from zintl family by using DFT [36]. The overall calculations were examined by means of (FP-LAPW) approach [37] as applied in the WIEN2k code [38]. The exchange–correlation potentials were determined by the help of generalized-gradient-approximation (GGA-PBE) [39]. The Only way to additionally improved the definiteness of explanation of d/f localized electrons is the usage of the spin-polarised (GGA + U) method [40], which further includes an on-site Coulomb repulsion. Further the wave functions in the interstitial region were expanded in plane waves with a cut off $(K_{max})^2 = (8/R_{MT})^2$. The muffin-tin radii ($R_{MT}$) are taken to be (2.5 a.u for Ca, 2.16 a.u for Zn, 1.92 a.u for Ge) elements respectively. The wave functions within muffin-tin spheres were expanded in spherical-harmonics with a cut off up to l_{max} = 10, whereas the charge density is Fourier expanded up to G_{max} = 12 atom unit (au)$^{-1}$. By using scalar-relativistic approach the value of $R_{MT} \times K_{max}$ was set to 7: R_{MT} refers to the smallest muffin-tin spheres (R_{MT}) radius in the unit cell, whereas k_{max} is the largest reciprocal lattice vector. The k integration over the Brillouin zone has purposed up to 1000 k points [41, 42] in the irreducible Brillouin Zone for $CaZn_2Ge_2$ compounds in ferromagnetic phase. In adition to this by using the semi-classical Boltzmann transport formalism which is implemented in Boltztrap code [43, 44] the thermoelectric properties have been investigated. A dense mesh of (100,000 k points) in the full Brillouin zone was utilized to obtain better result. Moreover the Quasi-harmonic Debye approximation [45], was used for the investigation of compound thermodynamic properties. The investigated formation energy is $0.91R_y$ as reported for said compound which depicts that the compound $CaZn_2Ge_2$ is thermodynamically stable due to its non-negative formation energy.

3 Result and discussions

3.1 Structural properties

The germinide based zintl compound $CaZn_2Ge_2$ exists in tetragonal geometry with space group *I4/mmm* (space group No. 139) and contain 1 Ca atom, 2 Zn atoms and 2 Ge atoms. The valence electrons present in the Ca(Ca$_1$) and Zn(Zn$_1$,Zn$_2$) atoms occupying the Wyckoff positions: (0,0,0) and ((0,0.5,0,25), (0.5,0,0.25)) respectively. While the Ge(Ge$_1$, Ge$_2$) atoms are located at the Wyckoff position ((0,0,0.384), (0,0,0.616)) as shown in Fig. 1. The compound structure behavior can easily be determined by investigating structure parameters. The relaxation of structural parameters of the material performed while utilizing the experimental data. Calculated structural parameters of the reported compound are noted in Table 1. Our noted theoretical values of lattice constant, bond angle and bond length are in good alignment with the experimental calculated values. Further the reported V_0, bulk modulus, pressure derivative of bulk modulus and ground state energy are depicted in Table 2. To the best of our knowledge, these are the first predicted values of the B and BP for the $CaZn_2Ge_2$ compound. With this comparatively low value of B, the understudy material

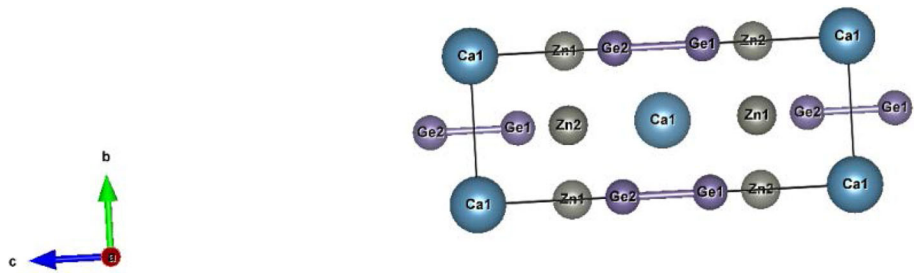**Fig. 1** Relaxed crystal structure of $CaZn_2Ge_2$ compound

Table 1 The calculated lattice constants a, b and c (in Å), and bond length d (in Å) for $CaZn_2Ge_2$ compound


Compound	Lattice constant		Bond Length
$CaZn_2Ge_2$	$a = b$	c	d_{Ge-Ge}
This work	4.12	10.83	2.43
Exp[a]	4.21	10.85	2.47

[a]Ref [1]

Table 2 Calculated values of V_0, B (GPa), Bp and E_0 (Ry) for $CaZn_2Ge_2$ compound in both AFM and PM Phase

Compound $CaZn_2Ge_2$	V_0	B(GPa)	BP	E_0
FM	674.5024	53.5510	5.0000	− 16,941.753661
PM	669.2030	57.6738	5.0000	− 16,941.725316

Fig. 2 Optimization plots showing energy verses unit cell volume of both PM and FM Phase for $CaZn_2Ge_2$ compound
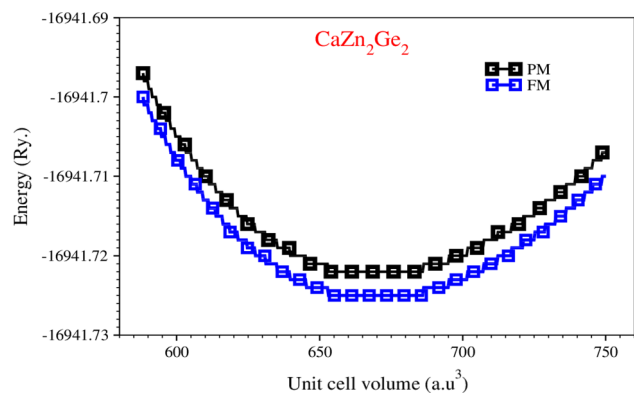

can be characterized as very soft material. By optimizing the volume of unit cell structure parameters (SP) of understudy compound were obtained. The unit cell energy is minimized by varying the volume of the cell. The volume of unit cell is optimized at a definite volume for the said compound known as optimized volume (V_0) of the material and the energy corresponding to V_0 is called ground state (GS) energy is reported in Table 2 while using two different phases. The graph between the unit cell volume and corresponding energies could be done by optimization process. Furthermore the optimization processes has been done to find out the exact ground state in two phases namely Paramagnetic (PM) and Ferromagnetic (FM) for the said compound. The optimization graph is shown in Fig. 2. From this optimized plot it is found that the Ferromagnetic (FM) configuration is the most suitable stable one with an optimized lattice parameter and higher noted volume. Moreover, the energy calculations of FM phase demonstrate the favorable nature of the FM configuration as compared to Paramagnetic (PM) phase with slightly more energetic stability under the PBE-GGA approximation.

3.2 Electronic properties

3.2.1 Chemical bonding

The Chemical nature of the material is established through deep understanding of Electron charge density. The exchange of charge among cations and anions is utilized to acknowledge the material ionic or covalent behavior. Electron charge density in (110) plane on the 3-D counter map of $CaZn_2Ge_2$ compound is shown in Fig. 3. Following Fig. 3, there is no evident sharing of charge density at the Ca–Zn and Ca–Ge bonding regions, the charge distribution around (Ca and Zn) and (Ca and Ge) are completely spherical which consequences the features of ionic bonding between Ca–Zn and Ca–Ge because of electro negativity differences between Ca (1.0), Zn (1.65) and Ge(2.01). While the dominant sharing with absent spherical appearance among Zinc (Zn) and Germinium(Ge) or in

Fig. 3 Charge density map on [110] plane of $CaZn_2Ge_2$ compound
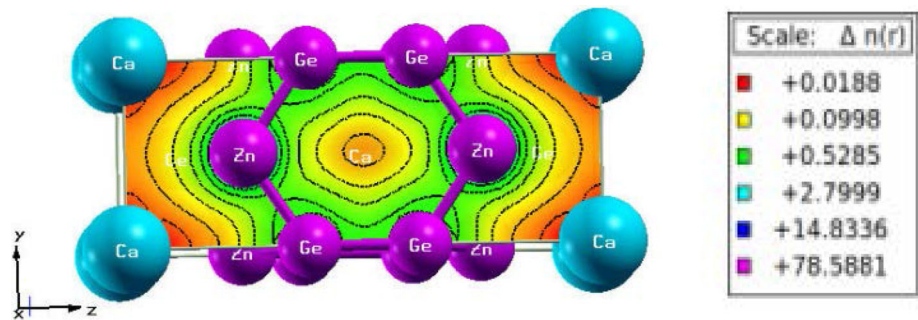
between Ge atoms are clearly observed depicting some covalent bonding nature. The strong hybridization present between Ca-d and Ge-p states are discussed in compound (Dos) plots. Overall, the compound $CaZn_2Ge_2$ shows mix ionic and covalent bonding nature.

### 3.2.2 Electronic band structure and density of states

The electronic behavior of a crystal can be described with the help of calculated electronic band structure and the density of states (DOS) which can give additional and thorough information. The energy band gap (E_g) of $CaZn_2Ge_2$ is calculated by GGA and GGA + U (U = 7 eV) approximations in both spin types. The Fermi level is set at the zero energy to be considered as a reference point for simplicity. The investigated band structures along the high symmetry directions, Γ, H, N, and (Γ,P) in the Brillouin zone are shown in (Fig. 4a, b).

The two valence band maximum shows the prominent dispersion along basal-plane Γ–H direction, while the rest of the other region shows dispersion along Γ–N and Γ–P direction indicating stronger conductivity in almost all directions. These two bands appear dominantly in both spin states while using the approximation (GGA and GGA + U) with a sharp peak appears in between high symmetry (Γ and H points) and wider peaks with shoulder appears at (H point) crossing the Fermi level and remain in the conduction band region of the understudy compound. While the conduction bands minimum remains in the conduction region and touch the Fermi level at high symmetry Γ point with further no overlapping is observed with the valence bands. In addition to this, at the same Γ point a direct band gap appears between the minima of conduction at the Fermi level and the maxima of the valence band below the Fermi level for the reported compound in both spin states using both approximation. This kind of multiband nature is a dominant favorable characteristic for thermoelectric materials.

In $CaZn_2Ge_2$, actually two valence band crossing the Fermi energy level at high symmetry H point and in between (Γ and H points) appeared in the band structures of both states through GGA and GGA + U. The conduction bands are completely filled and do not hold electrons. There is no energy gap in the Femi level, which indicates the pure metallic behavior whereas the spins up states are more closer to each other as compare to spin-down states in the Fermi level. So we could say that the closer states permit an easy mobility of electrons which further influence the conductivity of the system. Overall the compound $CaZn_2Ge_2$ shows full metallic nature due to the crossing mechanisms across the Fermi level as well as no energy band gap appears in both spin channels while using GGA and GGA + U approximations.

The (DOS) density of state function helps us to examine how much each (s/p/d/f) states contribute to conduction and valence bands. The investigations of DOS are plotted against energy in the range between − 5 to 5 eV for this compound using spin polarized GGA and GGA + U (U = 7 eV) approximations as shown in (Figs. 5, 6). The participations of electronic states and ions mechanisms are clearly understood by total and partial density of states ((TDOS) and (PDOS)) respectively.

However the total density of states curves shows metallic nature by intersecting the Fermi level in both spin up and down orientations for the $CaZn_2Ge_2$ compound by investigating through both approximations. Moreover the minor appearence in the valence band from the Fermi level towards a lower energy range through (GGA) and (GGA + U) approximations is of Ge-p state with no state contribution of the remaining atoms from the both spin states in the valence band region. While a dominant wide large spectra of Ca-d state appears in the conduction band from the Fermi level towards higher energy range between (1.5 and 4.5 eV) is clearly observed with the absent contribution of various states of remaining atoms in both up and down spin orientations in the conduction band region. A clear starting and shifting of d-state spectra towards further higher in energy is due to the use of (GGA + U) which actually treats localized d-shell electrons of the Ca atom. Overall, there is a strong hybridization between the minima of the valence band of Ge-p state and maxima of the conduction band of Ca-d state appear in both spin types through both approximations. These states are expected to be the major trend towards full metallic nature of the materials. Interestingly the appearance of Ca-d and Ge-p states spectra in both spin states are identical in both valence and conduction bands which indicates it fulfill frequently stoner argument [46] whereas the absence of remaining states over the entire energy range is reported in the said compound DOS plots while calculating through both (GGA and GGA + U) approximations.
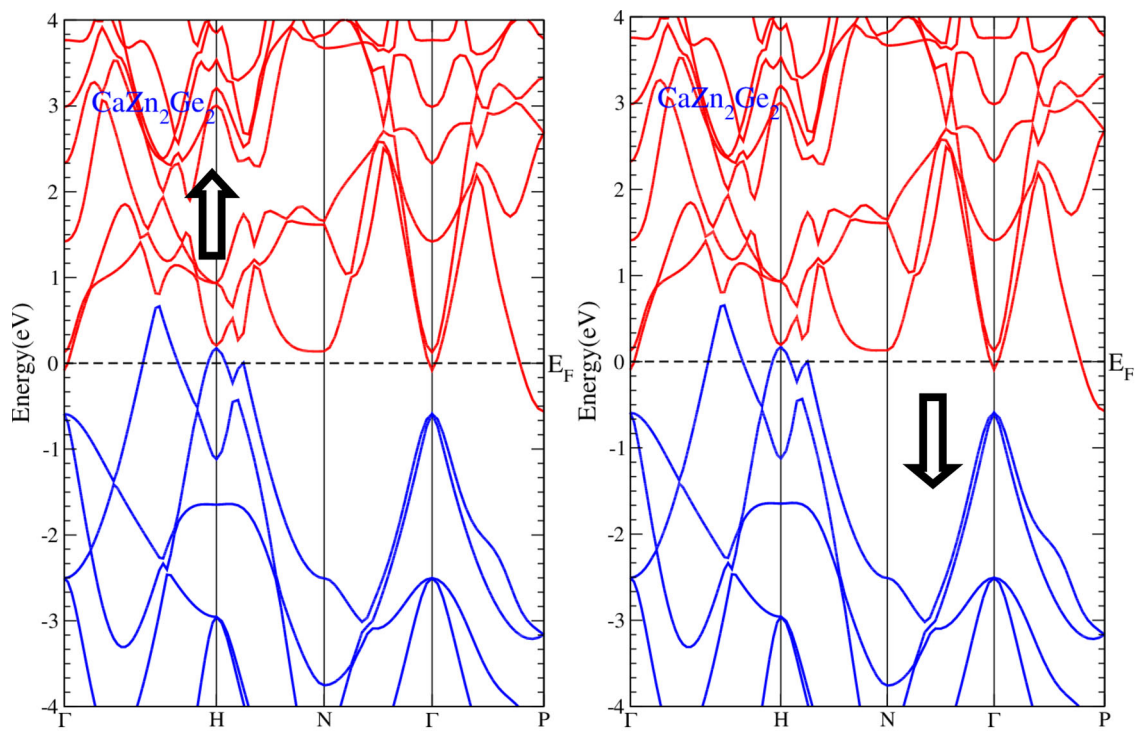
a Band structures of CaZn$_2$Ge$_2$ compound using GGA in both spin types
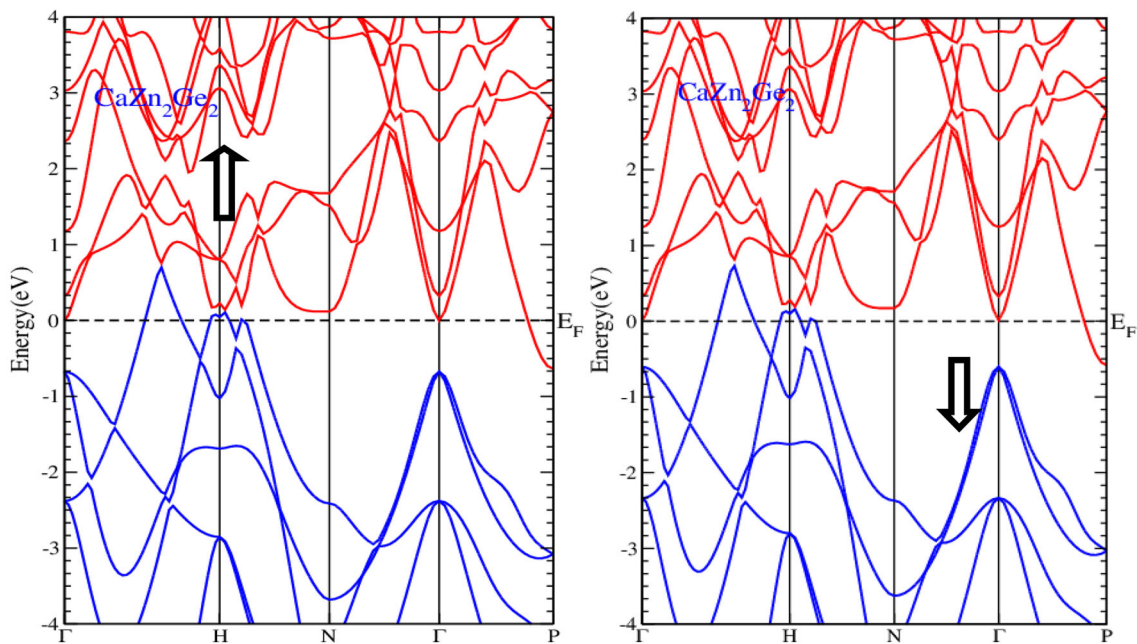
b Band structures of CaZn$_2$Ge$_2$ compound Using GGA+U (U=7eV) in both spin types

Fig. 4 a Band structures of CaZn$_2$Ge$_2$ compound using GGA in both spin types. **b** Band structures of CaZn$_2$Ge$_2$ compound Using GGA + U (U = 7 eV) in both spin types

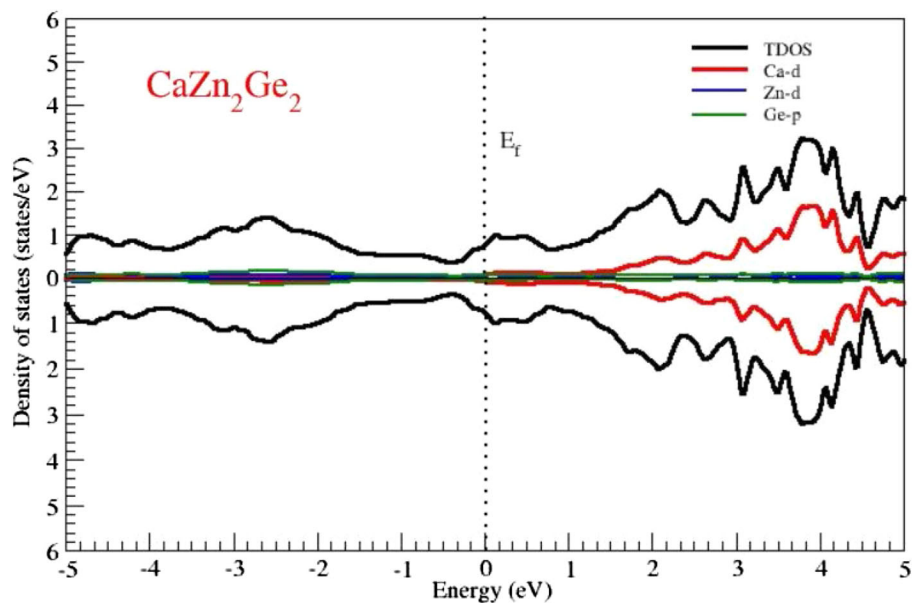**Fig. 5** DOS plot for $CaZn_2Ge_2$ compound using GGA in both spin up and down orientations

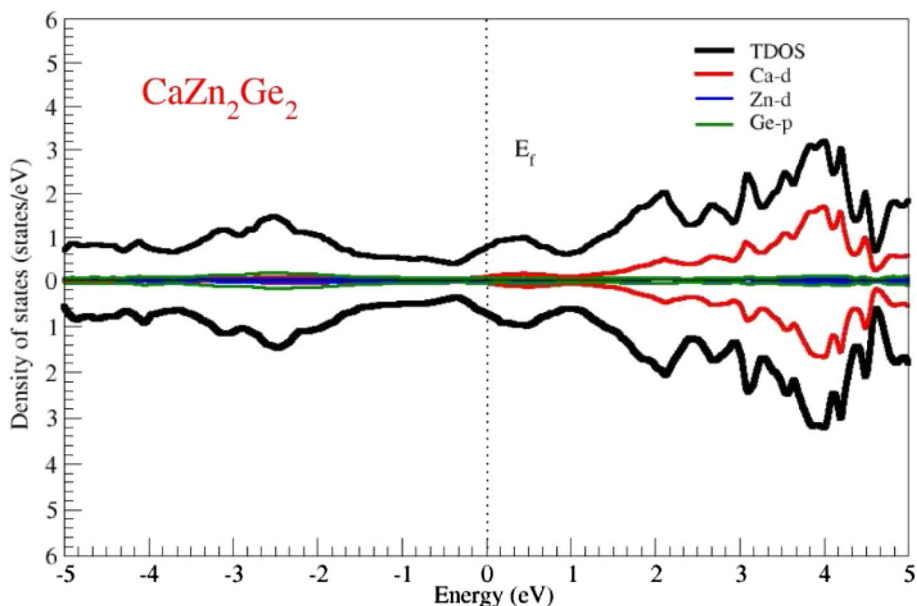**Fig. 6** DOS plot for $CaZn_2Ge_2$ compound using GGA + U (U = 7 eV) in both spin up and down orientations

Table 3 Magnetic moments of the interstitial region, individual atoms (Ca/Zn/Ge) and total cell for $CaZn_2Ge_2$ compound using GGA and GGA + U methods (in Bohr magnetrons μ_B)

Compounds	m^{instr}	M^{Ca}	M^{Zn}	M^{Ge}	m^c
(PBE-GGA)	(PBE-GGA)	− 0.00096	0.00011	0.00012	− 0.00428
GGA + U (U = 7 eV)	0.02706	0.00088	0.00250	0.00359	0.03014
Exp.	–	–	–	–	–
Other calc.	–	–	–	–	–

3.3 Magnetic properties

The results of the magnetic measurement like the $\mathbf{m^c}$ (total magnetic moment of each cell) of the compound along with their individual atomic (Ca, Zn and Ge) and interstitial magnetic moments of the compound $CaZn_2Ge_2$ by using GGA and GGA + U methods are reported in Table 3.

From this table, it is found that the Ge atom is the most contributing atom with positive value in the total cell magnetic moment as compared to other attached atoms in $CaZn_2Ge_2$ compound through both approximations. While the magnetic moment values of the interstitial region and individual (Ca and Zn) atoms show the peculiar behavior with a slight positive/negative contribution

Fig. 7 Variation of electrical conductivity (σ/τ) with temperature for CaZn$_2$Ge$_2$ compound
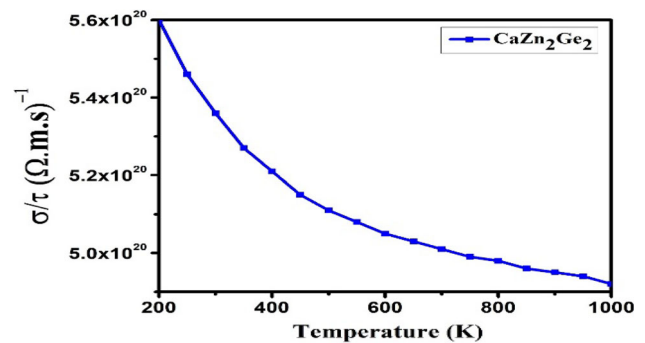
in the total cell magnetic moment by using GGA and GGA + U methods. The fundamental origin of magnetization comes from unoccupied Ca/Zn-d orbital.

The positive value of the magnetic moment through GGA + U indicates that the magnetic ground state for under study compound is ferromagnetic as shown in the optimization plot in Fig. 2, because it treats localized d-shell electrons of atoms and slightly increase its magnetic moment as compared to GGA in which the negative sign appeared. In addition to this, the calculated values of the magnetic moment through both approach especially at interstitial site and total cell for CaZn$_2$Ge$_2$ compound supports the net magnetic moment, while Zn/Ge opposes it. The opposite sign appears between the magnetic moments exhibit that, their valence band electrons interact in anti-ferromagnetic manner. This kind of behavior of the material originates from an anti-parallel orientation of the weak ferromagnetic moments present among atoms which clearly initiates weak ferromagnetism in the said compound.

3.4 Thermoelectric properties

The Thermoelectric material is said to be more efficient if it has a larger value of electrical conductivity and Seebeck coefficient while minor contribution of thermal conductivity for direct conversion of heat to electricity. In the present report, we have investigated Seebeck coefficient S, electrical (σ/τ) and thermal (k/τ) conductivity, power factor (PF) and Figure of merit (ZT) in the temperature range between 200 and 1000 K.

Electrical conductivity (σ/τ) is the transport of free charge carriers, which are observed in the plots of the said compound band structure and density of states. It is observed from the Fig. 7 that excited electrons play essential role in the electrical conductivity.

When the temperature initially increased, (σ/τ) curve started from the maximum value for the compound CaZn$_2$Ge$_2$ about 5.6 $\times 10^{20} (\acute{\Omega}.m.s)^{-1}$ and then decreased gradually over the entire mentioned temperature range and reach to its minimum value. At higher temperature electrons get more thermally excited due to higher thermal energy and can easily start its transport from high to low temperature region in a thermo-electric device. Because the collisions among electrons and positive metal ions become faster and thus increase in the resistivity along with relaxation time occur within a given temperature range, which leads to a clear decreasing trend in the compound CaZn$_2$Ge$_2$ electrical conductivity curve. Overall the variation of electrical conductivity with temperature shows an advancement and the increase of temperature causes a reduction in the quantity of carrier concentrations which as a result reduces the electrical conductivity.

In Fig. 8 the (k/τ) electronic thermal conductivity plot for CaZn$_2$Ge$_2$ compound is shown. Over the entire reported temperature range there is a clear linear increasing trend between the thermal conductivity and temperature. For a good thermo-electric material response, the value of thermal conductivity must exist in the lesser range. The (κ/τ) curve at temperature about 200 K initially started with the smaller value and then reach at its maximum value around 1.1 $\times 10^{16}$W/m.k.s at about 1000 K. The CaZn$_2$Ge$_2$ compound shows the dissimilar behavior in comparison with the plot shown by electrical conductivity (σ/τ) as depicted in Fig. 7. Moreover, the Wiedemann–Franz law cannot verify here between the electrical and thermal conductivity for this understudy compound where the trend between the plots is opposite, while the law demands the direct proportionality between the electronic thermal contribution and electrical conductivity [47].

A clear emperatur trend is observed in the Seebeck coefficient (S) curve over the mention temperature range as noticed from Fig. 9. The S is effected by temperature from its initial maximum value -2.25$\times 10^{-5}$ μV/K at about 200 K, when temperature further increases a gradual reduction of spectra in the negative region of (S) is seen up to 400 K where the CaZn$_2$Ge$_2$ compound shows n-type (the electronic transport is due to dominate electron charge carriers) nature till this temperature range, and then the compound spectra shows a smooth linear decreasing trend onward in temperature till 1000 K where the spectra (S) of compound further moved in the lower negative region showing pure n-type nature. Furthermore the said compound shows a negative values of Seebeck coefficient (S) in the observed temperature range. Overall the compound high negative (S) and higher electrical conductivity values lie below the room temperature, whereas the reported electronic thermal conductivity value is lower in the same temperature range.

The two main properties for the calculation of power factor term are Seebeck coefficient and electrical conductivity as depicted in Fig. 10. At temperature about 200 K the lowest value of power factor for CaZn$_2$Ge$_2$ compound is observed, further the electrical

Fig. 8 Variation of electronic thermal conductivity (k/τ) with temperature for CaZn$_2$Ge$_2$ compound
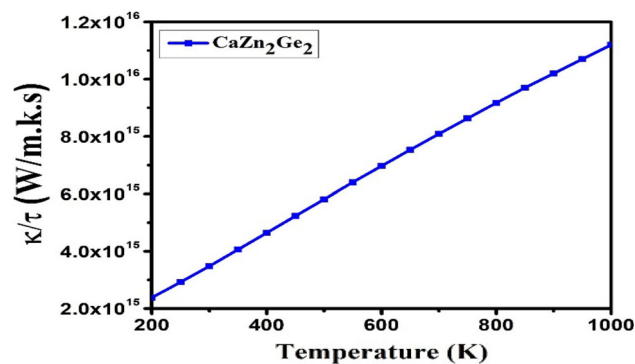

Fig. 9 Variation of Seebeck Coefficient (S) with temperature for CaZn$_2$Ge$_2$ compound
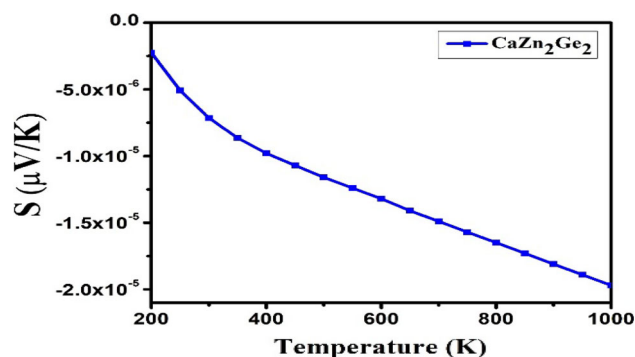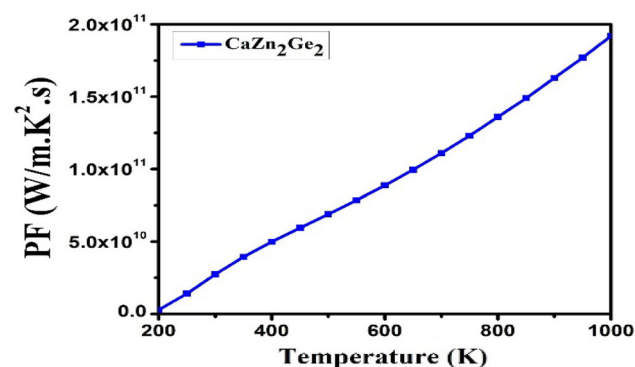

Fig. 10 Variation of Power Factor (PF) with temperature for CaZn$_2$Ge$_2$ compound

conductivity (σ) and Seebeck coefficient show their maximum values at the same temperature as reported in Figs. 7, 9. Whereas the highest value of power factor about 1.92×10^{11} (W/m.K^2.s) is noticed at 1000 K, which is a clear indication due to the comparatively low value of Seebeck coefficient and electrical conductivity in the high temperature region. Overall the curve of the power factor for the CaZn$_2$Ge$_2$ compound increases sharply below the room temperature till 400 K, but remains gradually increasing within the high temperature ranges.

The investigation of the temperature dependence of (ZT) figure of merits clearly defines the efficient thermo-electric material as presented in Fig. 11. The ZT curve linearly increased for CaZn$_2$Ge$_2$ compound till 400 K and at the same temperature below the room temperature about 200 K the lowest zero value of ZT for CaZn$_2$Ge$_2$ compound is observed just like PF, whereas the electrical conductivity (σ) and Seebeck coefficient as reported in Fig. 7, 9 show their maximum values at the same temperature. Further increase in a temperature value causes gradually increase the ZT curve where the compound finally attained its maximum value of (0.0171) at about 1000 K. So, the noticed high figure of merit (ZT) value is being just because of the maximum value of PF along with the fall in value of Seebeck and electrical conductivity at the mention range of temperature. Overall the whole thermo-electric parameters define the best possible response of the material applicability in both lower and higher temperature ranges especially in waste heat resource management.

Fig. 11 Variation of ZT with temperature for CaZn$_2$Ge$_2$ compound
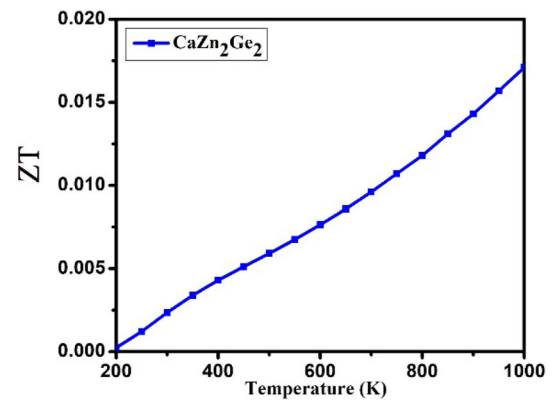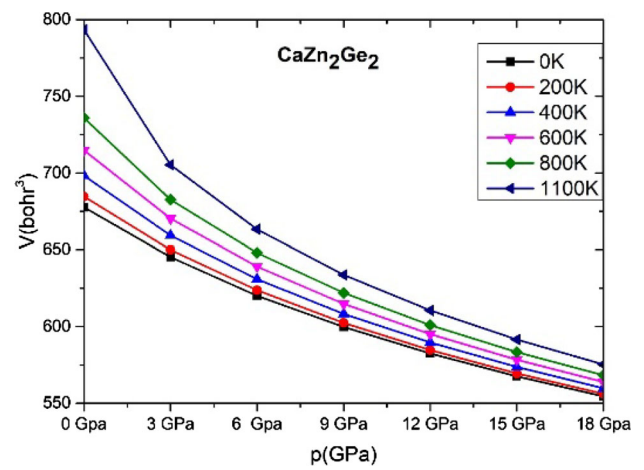

Fig. 12 Change in unit cell volume as a function of pressure and temperature for CaZn$_2$Ge$_2$ compound

3.5 Thermodynamic properties

In this report we have calculated the unit cell volume variation (V), Bulks modulus (B), the specific heat at constant volume (C$_v$) along with thermal expansion (α) and Debye temperature (θ_D) for the CaZn$_2$Ge$_2$ compound in the noticed pressure and temperature variations.

The variation in unit cell volume as a function of noted pressure and temperature ranges have mentioned in Fig. 12. It is obviously seen in all these curves that volume decreases with increasing pressure at a particular temperature whereas a dominant increase is found in volume with temperature enhancement at a particular pressure. So by increasing temperature unit cell volume increases along with the increase in inter-atomic distances while a clear reverse effect is seen with pressure. This trend is commonly found in almost all solids because with pressure enhancement compression is frequently experienced while temperature enhancement gives solid expansion.

The volume and bulk modulus are both strongly related with each other. The curves variation of bulks modulus with pressure and temperature have inverse impacts towards each other as noticed for volume variation. It tends to be seen from Fig. 13 that a reasonable increment in the bulk modulus with pressure along with a dominant decrease with temperature is seen at various temperature mentioned values. The clear increasing and decreasing pattern of B with pressure and temperature is just because of compression (the increase in the hardness) under pressure while expansion (the reduction in the hardness) under temperature.

The evolution of the specific heat at a constant volume (C$_V$) as a function of pressure at different temperature is depicted in Fig. 14. This is a significant thermodynamic property which gives complete information about the phase transition, vibrational properties etc. There is no such variation observed for the C$_V$ curve over the entire pressure range particularly at 0 K temperature while a clear decreasing escalation trends are observed for the rest of other mentioned temperature ranges. The figure indicates that the temperature variation has a greater impact than that of the pressure on the value of compound C$_v$ parameter. The C$_V$ curve initially started with the higher values of about (121.7324 Jmol^{-1} K^{-1} at 400 K), (123.526 Jmol^{-1} K^{-1} at 600 K), (124.1396 Jmol^{-1} K^{-1} at 800 K) and (124.5196 Jmol^{-1} K^{-1} at 1100 K) at about 0Gpa of pressure, moreover for these mentioned specific temperatures a clear minute decrease is observed further onward in the entire pressure range till 18Gpa for the compound CaZn$_2$Ge$_2$. Except at 200 K where it initially starts about 112.313 Jmol^{-1} K^{-1} which is our finding yielded value at 0Gpa and a gradual decrease is observed in higher pressure range.

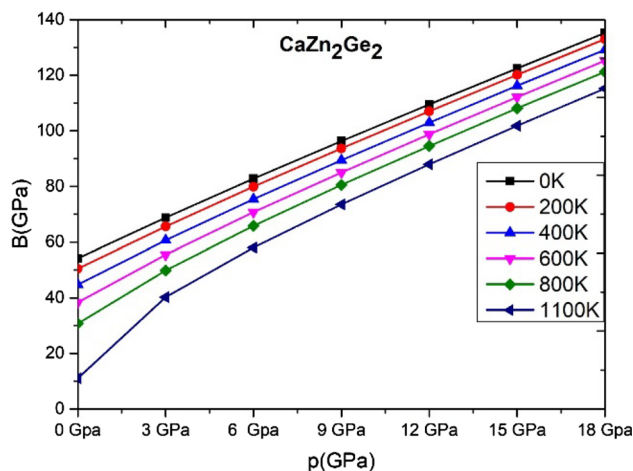**Fig. 13** Bulks Modulus (B) as a function of pressure and temperature for $CaZn_2Ge_2$ compound

Fig. 14 Nature of specific heat at constant Volume (C_v) with pressure and temperature for $CaZn_2Ge_2$ compound
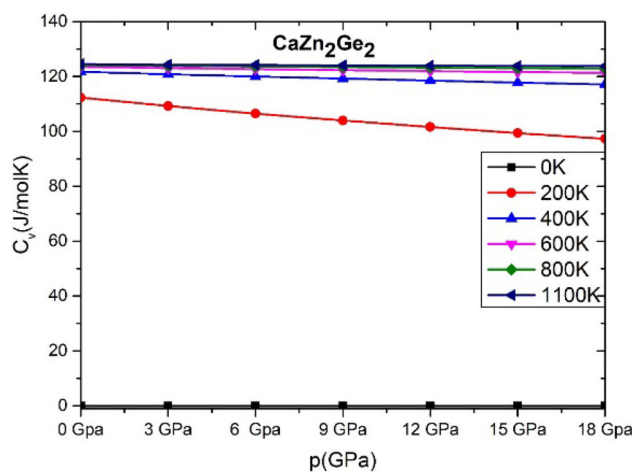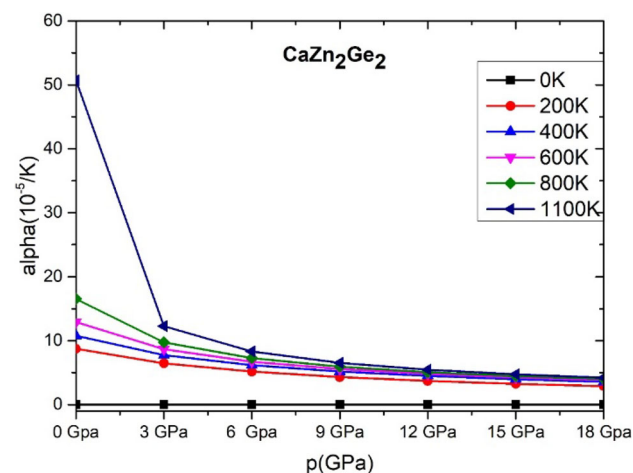

Fig. 15 Thermal expansion (α) with respect to pressure and temperature for $CaZn_2Ge_2$ compound

The variation of alpha (thermal expansion coefficient) with pressure and different temperature values is shown in Fig. 15. A clear decreasing trend is noticed over the entire pressure range in all the mentioned temperature values except at 0 K where the curve shows absent variation and remains stood at zero. A drastic decrease from its higher value in alpha for temperature of about 1100 K is clearly noticed till 3Gpa and then gradual decrease in value till 6Gpa and further almost constant decreasing trend onward in higher pressure range. Furthermore the temperature at about 400, 600 and 800 K all the three curves show gradually decreasing trend over the whole pressure range from 0 to 18Gpa. Overall the Pressure has an inverse trend with 'alpha', by increasing pressure 'alpha' falls almost rapidly.

Fig. 16 Debye Temperature (θ_D) as a function of pressure and temperature for $CaZn_2Ge_2$ compound
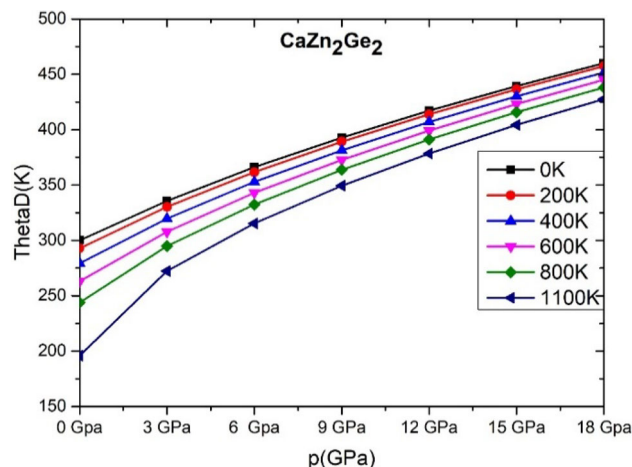

Figure 16 shows the curve of calculated ThetaD (Debye temperature) as a function of pressure at different temperature values. It can be seen that the ThetaD increases gradually over the entire pressure range from 0 to 18 Gpa while it decreases from lower to higher in different mentioned temperature. Moreover With increasing temperature, the growth rate of ThetaD becomes slow in comparison with the increment by increasing pressure. These thermodynamic outcomes of said compound may serve as significant informative reference for the future both theoretical as well as experimental studies for the other same class of compounds.

4 Summary

The structural, electronic, magnetic, thermoelectric and thermodynamic properties of $CaZn_2Ge_2$ compound from zintl family was examined under the frame work of density functional theory (DFT). The optimization results indicated that the Ferromagnetic (FM) configuration is the most suitable and stable one with an optimized lattice parameter and higher noted volume for the said compound. Band emperatu revealed metallic nature in both spin configurations, this is further validated by the electric conductivity results. The compound $CaZn_2Ge_2$ shows mix ionic and covalent bonding nature. The low magnetic moment of the compoundnusing the GGA + U scheme indicate the weak ferromagnetism. The maximum electrical conductivity (σ/τ) and negative seebeck coefficient (S) with the values $5.6 \times 10^{20}(\acute{\Omega}.m.s)^{-1}$ and -2.25×10^{-5} µV/K were reached below the room emperature while maximum ZT with a value 0.0171 and power factor were achieved at 1000 K for the said compound. These finding of material to both low and high temperature increase the use of its demand in waste heat management. The bulk modulus and Debye temperature increases with the increase in temperature, while unit cell volume, specific heat at constant Volume and Thermal expansion decreased with the increase in termature.

References

1. C. Kranenberg, D. Johrendt, A. Mewis, R. Pöttgen, G. Kotzyba, H. Trill, B.D. Mosel, J. S. S. Chem. **167**(1), 107–112 (2002)
2. G. Murtaza, N. Yousaf, M. Yaseen, A. Laref, S. Azam, Mater. Res. Express **5**, 016304 (2018)
3. J. Sun, D.J. Singh, J. of Mate. Chem. A **5**, 8499–8509 (2017)
4. F. Gas, S. Ottensmann, D. Stark, S.M. Haïle, G.J. Snyder, Adv. Funct. Mater **15**, 1860–1864 (2005)
5. A.A. Khan, M. Yaseen, A. Laref, G. Murtaza, Phys. B Condensed Matter. **541**, 24–31 (2018)
6. E.S. Toberer, A.F. May, B.C. Melot, E. Flage-Larsen, G.J. Snyder, Dalton Tran. **39**, 1046–1054 (2010)
7. A.A. Khan, A.U. Rehman, A. Laref, M. Yousaf, G. Murtaza, Zeitschrift für Natur. A **73**(10), 965–973 (2018)
8. A. Grytsiv, A. Leithe-Jasper, H. Flandorfer, P. Rogl, K. Hiebl, C. Godart, T. Velikanova, J. Alloys Comp. **266**(1–2), 7–12 (1998)
9. Z. Zada, H. Ullah, R. Bibi, S. Zada, A. Mahmood, Zeitschrift für Natur. A **75**(6), 543–549 (2020)
10. P. Pearon, L. Calvert, *Pearson's Handbook of Crystallographics data for Intermetallic Phases* (ASM international, Metals park, 1991)
11. Z. Ban, M. Sikirica, Acta. Crystallogr. **18**, 594 (1965)
12. W. Jeitschko, R. Glaum, L. Boonk, J. Solid State Chem. **69**, 93 (1987)
13. R. Nagarajan, E.V. Sampathkumaran, L.C. Gupta, R. Vijayaraghavan, V. Prabhabwalkar, B. Padalia, Phys. Lett. A **84**, 275 (1981)
14. L. Eyring, K.A. Gschneidner, G.H. Lander, *Handbook on the Physics and Chemistry of Rare Earths* (Elsevier, Amsterdam, 2002)
15. M. Reehuis, W. Jeitschko, J. Phys. Chem. Solids **51**, 961 (1990)
16. B. Ni, M.M. Abd-Elmeguid, H. Micklitz, J.P. Sanchez, P. Vulliet, D. Johrendt, Phys. Rev. B **63**, 100102–100111 (2001)
17. K. Masumoto, W.A. McGahan, Electromagnetic applications of intermetallic compounds. MRS Bull. **21**(5), 44–49 (1996)
18. R. Bibi, Z. Zada, A.A. Khan, S. Azam, M. Irfan, B.U. Haq, S.A. Khan, J. Solid State Chem. **302**, 122388 (2021)

19. Z. Zada, H. Ullah, R. Zada, S. Zada, A. Laref, S. Azam, M. Irfan, Phy. B: Condensed Mat. **607**, 412866 (2021)
20. G. Murtaza, A.A. Khan, M.M. AL-Anazy, A. Laref, Q. Mahmood, Z. Zada, M. Aman, Eur. Phys. J. Plus **136**(2), 1–16 (2021)
21. Z. Zada, H. Ullah, R. Zada, A.A. Khan, A. Mahmood, S.M. Ramay, Eur. Phys J. Plus **136**(4), 1–12 (2021)
22. L.M. Schetky, Miscellaneous applications of intermetallic compounds. MRS Bull. **21**(5), 50–55 (1996)
23. Z. Zada, A. Laref, G. Murtaza, A. Zeb, A. Yar, Int. J. Mod. Phys. B **33**(18), 1950199 (2019)
24. M.I. Katsnelson, V.Y. Irkhin, L. Chioncel, A.I. Lichtenstein, R.A. De Groot, Rev. Moden. Phys. **80**(2), 315–378 (2008)
25. H. Atsufumi, T. Koki, J. Phys. D **47**, 193001 (2014)
26. D. Johrendt, C. Felser, O. Jepsen, O.K. Andersen, A. Mewis, J. Rouxel, J. Solid State Chem. **130**, 254 (1997)
27. A. Wurth, D. Johrendt, A. Mewis, C. Huhnt, G. Michels, M. Roepke, W. Schlabitz, Z. Anorg, Allg. Chem. **623**, 1418 (1997)
28. V. Keimes, D. Johrendt, A. Mewis, C. Huhnt, W. Schlabitz, Z. Anorg, Allg. Chem. **623**, 1699 (1997)
29. C. Huhnt, G. Michels, M. Roepke, W. Schlabitz, A. Wurth, D. Johrendt, A. Mewis, Phys. B **240**, 26 (1997)
30. C. Huhnt, W. Schlabitz, A. Wurth, A. Mewis, M. Reehuis, Phys. Rev. B **56**, 13796 (1997)
31. C. Huhnt, W. Schlabitz, A. Wurth, A. Mewis, M. Reehuis, Physica B **252**, 44 (1998)
32. V. Keimes, A. Hellmann, D. Johrendt, A. Mewis, Z. Anorg, Allg. Chem. **624**, 830 (1998)
33. A.T. Karim, M.A. Hadi, M.A. Alam, F. Parvin, S.H. Naqib, A.K.M.A. Islam, J. Phy. Chem. Solids **117**, 139–147 (2018)
34. M.A. Hadi, M.S. Ali, S.H. Naqib, A.K.M.A. Islam, Chinese Physics B **26**(3), 037103 (2017)
35. Z. Zada, A.A. Khan, A.H. Reshak, M. Ismail, S. Zada, G. Murtaza, J. Bila, J. Mole, Structure **1252**, 132136 (2021)
36. P. Hohenberg, W. Kohn, Phys. Rev. **136**, B864-871 (1964)
37. W. Kohn, L.J. Sham, Phys. Rev. **140**, A1133-1138 (1965)
38. P. Blaha, K. Schwarz, G. K. Madsen, D. Kvasnicka, J. Luitz, wien2k, An augmented plane wave+ local orbitals program for calculating crystal properties, ISBN 3–9501031–1–2, (2001)
39. J.P. Perdew, K. Burke, M. Ernzerhof, Phys. Rev. Lett. **77**, 3865 (1996)
40. A.I. Liechtenstein, V.I. Anisimov, J. Zaanen, Phys. Rev. B **52**, R5467 (1995)
41. O. Bengone, M. Alouani, P. Blochl, J. Hugel, Phys. Rev. B **62**, 16392 (2000)
42. H.J. Monkhorst, J.D. Pack, Phys. Rev. B **13**, 5188–5192 (1976)
43. J.D. Pack, H.J. Monkhorst, Phys. Rev. B **16**, 1748–1749 (1977)
44. G.K.H. Madsen, J. Am. Chem. Soc. **128**, 12140 (2006)
45. E. Francisco, M.A. Blonco, G. Sanjurjo, Phys. Rev. B **63**, 049107 (2001)
46. M.C. Sahnoun, O. Daul Haas, A. Wokaun, J. Phys. Condense. Matter **17**, 7995 (2003)
47. X. Du, L. Mihaly, P.B. Allen, Phys. B **194–196**, 1507–1508 (1994)